

Cite this: *RSC Adv.*, 2018, **8**, 14414

## Laccase immobilization and surface modification of activated carbon fibers by bio-inspired poly-dopamine

Chencheng Zhang,<sup>id ab</sup> Lili Gong,<sup>c</sup> Qinghui Mao,<sup>b</sup> Pingfang Han,<sup>\*a</sup> Xiaoping Lu<sup>a</sup> and Jiangang Qu<sup>b</sup>

In this study, we developed a new synthesis method for modifying activated carbon fibers (ACFs) by dopamine with oxidation-based self-polymerization (DA-ACFs). In addition, laccase was immobilized on the surface of unmodified ACFs (L-ACFs) and DA-ACFs (LDA-ACFs) via cross-linking after being incubated for 12 h at 5 °C. The surface composition and microstructure of the samples were characterized by scanning electron microscopy, X-ray photoelectron spectroscopy, attenuated total reflectance Fourier-transform infrared reflection and thermo-gravimetric analysis. The optimized laccase concentration for preparing the samples was 2.0 g L<sup>-1</sup>. The results demonstrated that the successful poly-dopamine modification increased the catalytic abilities of the ACFs in terms of biocompatibility and hydrophilicity. Compared with free laccase, the immobilized laccase exhibited significantly higher relative activity over a pH range of 3.5–6.5 and a temperature range of 30–60 °C; the thermo-stability increased, and 50% relative activity of the LDA-ACFs remained after 5 h at 55 °C. After six cycles of reuse, the relative activity of LDA-ACFs remained ≥60%, compared to 40% activity remaining for L-ACFs, and long-term storage stability was demonstrated. Moreover, the kinetic parameters ( $K_m$ ) of the two immobilized laccases were both higher than that of free laccase, whereas the maximum velocities ( $V_{max}$ ) were lower. These results indicate that the DA-ACFs are economical, simple, and efficient carriers for enzyme immobilization, and can be suitable for further biotechnology and environmental applications.

Received 12th February 2018

Accepted 22nd March 2018

DOI: 10.1039/c8ra01265b

rsc.li/rsc-advances

## Introduction

As a family of multi-copper oxidases, laccases have been developed as catalytic agents that can be used for water-based treatment of aromatic and non-aromatic compounds,<sup>1</sup> such as in lignin valorization,<sup>2</sup> organic synthesis,<sup>3</sup> dye discoloration,<sup>4</sup> and wastewater detoxification.<sup>5</sup> However, laccases are not desirable for large-scale applications owing to certain properties of free enzymes, including their sensitivity to denaturing agents and non-reusability.<sup>6</sup> One way to overcome these limiting factors is to immobilize laccases on various carriers, which can protect them from denaturation, improve their stability, maintain good catalytic efficiency, and lead to more economical processes.<sup>7–10</sup> Thus, it is important to choose an appropriate carrier to optimize immobilization, including pore size, chemistry of the anchor group, specific surface area, and biodegradability.<sup>11–14</sup>

Furthermore, strategies where laccase physically adsorbed and immobilized by cross-linking to various supports are most

commonly used for immobilization.<sup>15,16</sup> In contrast to covalent attachment, enzyme immobilization *via* adsorption is generally too weak to keep the enzyme fixed to the carrier, especially under industrial conditions.<sup>17</sup> Consequently, increasing interest has arisen in covalent attachment, in that covalent bonding makes the enzyme more stable and attractive for industrial applications.<sup>18</sup>

Activated carbon fibers (ACFs) have attracted substantial research interest because of their high surface areas, various functional groups, narrow pore-size distributions, and broad availability of raw material sources.<sup>19,20</sup> Therefore, ACFs show great potential for application as immobilization carriers. For example, Zuo *et al.*<sup>21</sup> used an ACF as a carrier to prepare composite materials by loading a biological enzyme on the surface to remove formaldehyde. More recently, increased attention has been paid to developing optimal methods for modifying ACFs, such as oxidation treatment, plasma treatment, thermal treatment, and amino-functionalization for introducing oxygen/nitrogen-containing functional groups.<sup>22–25</sup>

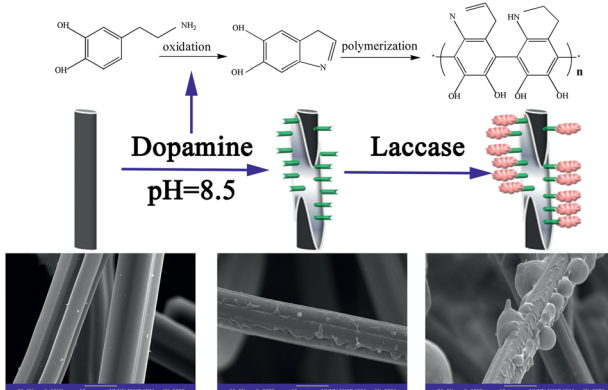
Some recent data have shown that the adhesion capacity of enzymes could be improved using a material surface with moderate hydrophilicity.<sup>26</sup> Wang *et al.*<sup>27</sup> reported that HNO<sub>3</sub> oxidation is a favorable surface treatment for carbon fiber carriers, providing a promising method to prepare

<sup>a</sup>Biotechnology and Pharmaceutical Engineering, Nanjing Tech University, Nanjing 210009, PR China. E-mail: hpf@njtech.edu.cn

<sup>b</sup>College of Textile and Garment, Nantong University, Nantong 226019, PR China

<sup>c</sup>Nantong Health College of Jiangsu Province, Nantong 226007, PR China





Scheme 1 Preparation of LDA-laccase.

biocompatible materials as immobilized bio-carriers. However, the application of ACFs has been limited by poor adhesion properties due to their smooth surface, so that the interaction between carriers and enzymes is relatively unsatisfied. Thus, the biological compatibility of the carbon surface must be enhanced by doping it with a moiety such as a hydroxyl group, amino group, or aldehyde group.<sup>28</sup>

Dopamine (DA, 3,4-dihydroxyphenethylamine) is a well-known molecular bio-mimetic adhesive, that can interact with nearly all types of surfaces owing to its self-polymerization, high biocompatibility, and hydrophilicity.<sup>29,30</sup> Yang *et al.*<sup>31</sup> demonstrated an approach of combining DA and titanium(IV) that can be considered an excellent supporter for enzyme immobilization owing to the presence of hybrid nano-particles.

In our previous work, we successfully immobilized ACFs with laccase.<sup>32</sup> The main goal of the present study was to investigate the effect of DA modification on the surface of ACFs (DA-ACFs) *via* bio-mimetic coating, using the prepared synthesized materials as carriers to immobilize laccase (LDA-ACFs) by cross-linking (Scheme 1). The attractive aspect of this immobilization technique is that the binding force between the enzyme and the functional group on the surface of the carrier is strong, while can still possess good stability, as compared with conventional techniques. To our knowledge, this is the first study to explore the feasibility of immobilizing an enzyme on DA-ACFs. The activity, thermal stability, pH stability, storage stability, and reusability of the LDA-ACFs compared to the free enzyme were investigated in detail. The morphology of the synthesized materials was characterized using scanning electron microscopy (SEM). The chemical composition of the modified DA-ACFs was estimated by X-ray photoelectron spectroscopy (XPS), attenuated total reflectance Fourier-transform infrared reflection (ATR-FTIR), and thermo-gravimetric (TG) analysis. Overall, we demonstrated that the DA-ACFs have advantageous attributes in terms of high efficiency and improved stability for laccase immobilization, showing great potential for practical applications.

## Experimental

### Materials

ACFs were prepared by the carbonization of viscose fibers supplied by Nantong Sutong Carbon Fiber Co. Ltd. (Jiangsu, China) under a nitrogen flow ( $10\text{ }^{\circ}\text{C min}^{-1}$  up to  $600\text{ }^{\circ}\text{C}$ , held for 2 h, and finally cooled down to room temperature). A fungal laccase from *Aspergillus* (Ruibo L8598,  $\geq 100\text{ U g}^{-1}$ ) and bovine serum albumin were provided by Bomei Company (Anhui, China). Dopamine hydrochloride, 2,2'-azino-bis (3-ethyl benzothiazoline-6-sulfonic acid) (ABTS), and tris (hydroxymethyl) methyl amino methane were purchased from Meryer Chemical (Shanghai, China). Deionized water was used throughout the experiments and all other reagents were of analytical grade.

### Preparation of modified ACFs

A sample of ACFs was prepared following a common method, as reported previously.<sup>32</sup>  $\text{HNO}_3$ -treated ACFs were then dispersed in a solution of  $1.0\text{ g L}^{-1}$  DA in deionized water at  $25\text{ }^{\circ}\text{C}$ . The pH of the solution was adjusted to 8.5 by adding Tris and confirmed with a pH meter (S-25, REX instruments, Shanghai, China). The ACFs were coated with insoluble polymers under moderate mechanical stirring for 6 h. The resulting products were washed with deionized water until the solution became transparent and colorless, collected by centrifugation (4000 rpm, 5 min), and dried overnight in a vacuum oven at  $50\text{ }^{\circ}\text{C}$ .

### Instrumentation

The microstructure morphologies were observed by SEM (KYKV-2800, KYKY Technology Co., Ltd., Beijing, China) at an accelerating voltage of 20 kV, and after sputtering the sample surfaces with a thin layer of gold. The chemical composition of the prepared ACF composite was determined by XPS (ESCALAB 250XI, Thermo Electron Corporation, USA). The surface functional groups of the prepared ACF composites were determined by FTIR (IS10, Thermo Fisher, USA) in the region of  $600\text{--}4000\text{ cm}^{-1}$ , using an attenuated total reflectance (ATR) accessory with a diamond crystal. The wettability was observed by using a contact angle-measuring device (JC2000C, Powereach, Shanghai, China). Thermal analyses were conducted by TG analysis using a thermo-microbalance (TG209F3, NETZSCH, Germany) in the temperature range of  $40\text{--}800\text{ }^{\circ}\text{C}$ , with heating at a rate of  $10\text{ }^{\circ}\text{C min}^{-1}$ . The experiments were performed under a nitrogen atmosphere ( $30\text{ mL min}^{-1}$ ).

### Immobilization of laccase on the DA-ACFs

Two grams of DA-ACFs was suspended in 20 mL buffer ( $\text{Na}_2\text{HPO}_4\text{--C}_6\text{H}_8\text{O}_7$ , 0.5 M, pH 5.0) containing  $2.0\text{ g L}^{-1}$  laccase and stirred with mechanical agitation of 200 rpm at  $5\text{ }^{\circ}\text{C}$  for 12 h. The products were centrifuged and then washed with buffer (0.1 M, pH 5.0) three times until no enzymatic activity was detected in the supernatant, dried in a vacuum freeze-dryer, and stored in a fridge at  $5\text{ }^{\circ}\text{C}$  for future use.



## Determination of laccase activity

The activities of free and immobilized laccase were measured using ABTS as a standard in buffer (0.5 M, pH 5.0).<sup>33</sup> The reaction mixture was incubated for 10 min at 30 °C, and then analyzed by measuring the absorbance increase at 420 nm with a visible spectrophotometer (V-1200, MAPADA, Shanghai, China). The relative activity of enzyme was calculated using eqn (1):<sup>34</sup>

$$\text{Relative activity \%} = \frac{A_i}{A_f} \times 100 \quad (1)$$

where  $A_i$  is the activity of immobilized laccase, and  $A_f$  is the activity of free laccase under similar experimental ( $U = 102 \pm 4 \text{ U g}^{-1}$ ).

The Coomassie Brilliant Blue method was used to determine the effect of the laccase concentration on the immobilization efficiency. The laccase concentration was changed between 0.5–5.0 g L<sup>-1</sup> in the buffer (0.5 M, pH 5.0), the solution was incubated at 5 °C for 12 h, and the enzyme loading rate was calculated using eqn (2) from a previous study:<sup>35</sup>

$$\text{Enzyme loading rate (\%)} = \frac{(C_i V_i - C_f V_f)}{W_a} \times 100 \quad (2)$$

where  $C_i$  and  $C_f$  are the initial and final concentrations of laccase (g L<sup>-1</sup>), respectively,  $V_i$  is the initial volume of laccase solution (L),  $V_f$  is final volume of laccase solution (L), and  $W_a$  is the mass of support samples (g).

In a 10 mL centrifuge tube, 2 mL of different buffer solutions (0.1 M, pH 2.0–8.0) was mixed with 1 mL of free laccase (0.2 g L<sup>-1</sup>) or 1 g of immobilized laccase and incubated at 30 °C for 30 min. Then, 2 mL of ABTS solution was added and the reaction mixture was held for 5 min at 30 °C. Similarly, the effect of temperature on the laccase activity was measured over a range of 25–80 °C at a pH of 5.0 for 30 min. The storage stability of the laccase immersed in buffer (0.1 M, pH 5.0) was investigated at 4 °C for various durations. Thermal stability was measured at 55 °C and reusability of the immobilized laccase was also assessed. All enzymatic activity assays were performed three times.

The Michaelis–Menten kinetic parameters of free and immobilized laccase were measured with ABTS in the range of 0.4–5.0 mg mL<sup>-1</sup> in buffer solutions under the optimal conditions, and estimated according to Lineweaver–Burk plots fit to the following eqn (3):<sup>33</sup>

$$\frac{1}{V} = \frac{K_m}{V_{\max}} \times \frac{1}{[S]} + \frac{1}{V_{\max}} \quad (3)$$

where  $V$  (mg (mL min)<sup>-1</sup>) is the catalytic reaction rate,  $V_{\max}$  is the maximum rate of the reaction,  $[S]$  is the concentration of substrate, and  $K_m$  is the Michaelis–Menten constant.

## Results and discussion

### Surface morphology of the samples

The surface morphologies of ACFs before and after treatment were observed by SEM. As shown in Fig. 1a and b, the surfaces of pristine ACFs were smooth, whereas the surfaces of DA-ACFs

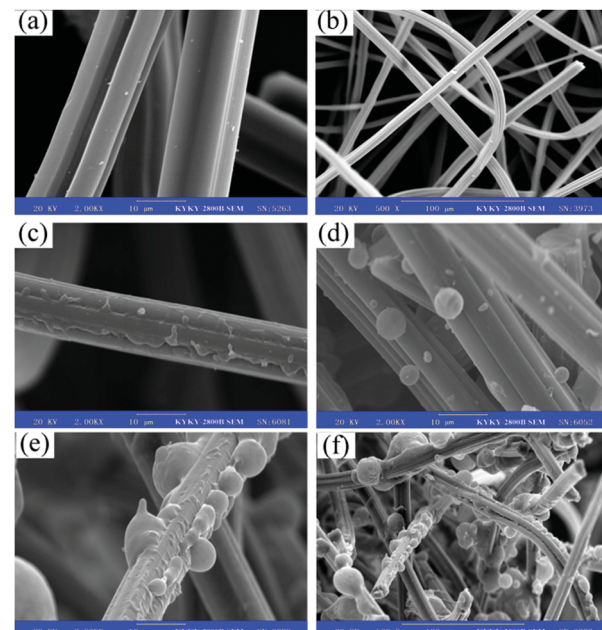


Fig. 1 SEM images of fibers: (a and b) the pristine ACFs, (c) DA-ACFs, (d) L-ACFs, and (e and f) LDA-ACFs.

exhibited a distinct rough layer that was deposited after DA oxidative self-polymerization. The SEM images of the ACFs and DA-ACFs with immobilized laccase are shown in Fig. 1e and f. Many spherical particles were evenly dispersed on fibers and surfaces of the DA-ACFs, which could be attributed to the greater amount of proteins in the DA solution.<sup>36</sup> This property could help support laccase adherence to the surface.

### Surface chemical composition of the ACF samples

The successful surface modification of ACFs was further ascertained by XPS. Fig. 2 shows the XPS wide-scan view, demonstrating the core-level C 1s of pristine ACFs and DA-ACFs, and the core-level N 1s of the DA-ACFs. Fig. 2a and Table 1 show different chemical states of elemental C, O, and N in the

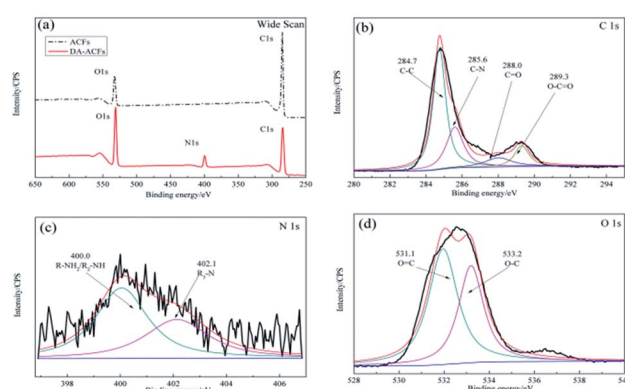


Fig. 2 XPS spectra of microspheres before and after modification: (a) wide scan, (b) C 1s of ACFs, (c) C 1s of DA-ACFs and (d) N 1s of DA-ACFs.

Table 1 Elemental contents on the surface of the samples

Sample	Atom content (%)		
	C 1s	O 1s	N 1s
ACFs	84.68	13.87	1.45
DA-ACFs	63.67	26.73	9.6
LDA-ACFs	60.34	38.03	1.63

deconvoluted core-level spectra due to the complicated nature of poly-dopamine on ACFs. As shown in Fig. 2b, the C 1s spectrum of the ACF surface contains two peak components: one for the C-C species at a BE of  $\sim 284.9$  eV, and the other for carboxyl (O-C=O) species at a BE of  $\sim 288.6$  eV. The C 1s core-level spectrum of DA-ACFs could be curve-fitted with three peak components showing BE values at  $\sim 283.4$  eV for C-C species,  $\sim 285.0$  eV for C-N species, and  $\sim 288.7$  eV for O-C=O species, which were introduced by the DA oxidative self-polymerization (Fig. 2c).

Fig. 2b also demonstrates few C-O bonds in the pristine ACF samples. However, after self-polymerization, the contents of different oxygen-containing bonds changed drastically. According to the spectra, the N 1s deconvoluted into two different types of N-containing species, one at  $\sim 398.7$  eV for  $-N=$  and another at  $\sim 400.1$  eV for N-H. The additional peak of C-O species and the peaks of N 1s indicated the presence of the poly-dopamine layer on the surface of ACFs (Fig. 2c and d).<sup>37</sup>

As shown in Fig. 3b, after the enzyme was immobilized by cross-linking, the C 1s spectrum was deconvoluted into four peaks at  $\sim 284.7$  eV for the C-C species,  $\sim 285.8$  eV for the C-N species,  $\sim 285.8$  eV for the O-C=O species, and a new peak for the C=O stretching molds at  $\sim 288.0$  eV. In addition, the N 1s component (Fig. 3c) at  $\sim 400.0$  eV corresponded to the R-NH<sub>2</sub>/R<sub>2</sub>-NH species and a peak at  $\sim 402.1$  eV was detected for the R<sub>3</sub>-N species owing to the presence of the O 1s component (Fig. 3d), which was attributed to the functional groups of the proteins present.<sup>33</sup> It is notable that strong bonds were detected between dopamine and laccase, presumably reflecting reactions between quinone of poly-dopamine and amines, sulphydryl, and imidazole groups in the proteins.<sup>38</sup> In addition, the differences

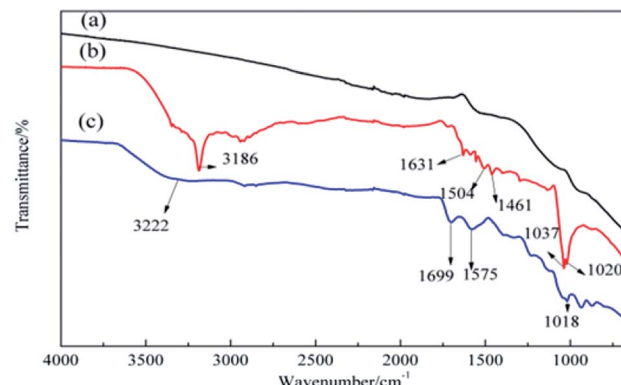


Fig. 4 ATR-FTIR spectra of (a) ACFs, (b) DA-ACFs, and (c) LDA-ACFs.

shown in Fig. 1b and f indicated that the self-polymerization modification increased the quantity of immobilized laccase with the DA modification on ACFs, which clearly revealed the successful immobilization of laccase on ACFs with high enzyme loading.

Moreover, ATR-FTIR was used to analyze the chemical structure of pristine ACFs, DA-ACFs, and LDA-ACFs. As shown in Fig. 4b, the peaks at  $3186\text{ cm}^{-1}$  and  $1631\text{ cm}^{-1}$  were assigned to N-H and C=N stretching vibrations, the adsorption peaks at  $1504\text{ cm}^{-1}$  and  $1461\text{ cm}^{-1}$  were assigned to the N-H and C-N stretching bands that may reflect stretching of the benzene ring in poly-dopamine, and the peaks at  $1037\text{ cm}^{-1}$  and  $1020\text{ cm}^{-1}$  were assigned to the C-O-C stretching bands.<sup>39</sup> After immobilizing with laccase, peaks at  $3222\text{ cm}^{-1}$ ,  $1699\text{ cm}^{-1}$ ,  $1575\text{ cm}^{-1}$ , and  $1018\text{ cm}^{-1}$  were observed when analyzing the structure of acylamine.<sup>40</sup> Moreover, the peak changes (Fig. 4b) were largely consistent with the XPS results (Fig. 2c and d), confirming that DA was coated on the surfaces of ACFs through oxidative self-polymerization, and the spectra (Fig. 4c and 3) implied that fibroin proteins had been successfully grafted onto the ACFs *via* immobilization.

### Wettability behavior of the ACF samples

The wetting property of ACFs is important for enzyme immobilization. Thus, the wettability of the samples was determined by performing contact-angle measurements. As shown in Fig. 5a and 2  $\mu\text{L}$  droplet of deionized water firmly held by ACFs and the contact angle was approximately  $180^\circ$ , since ACFs are hydrophobic and have a carbon structure with low oxygen content on their surfaces (Fig. 4a). When a droplet was placed on the surface of DA-ACFs, it spread out quickly and was absorbed less than 1 s (Fig. 5b). These data indicated that the surface of DA-ACFs was hydrophilic.<sup>41</sup> Probing the hydrophilicity of ACFs in water and aqueous solutions is particularly important for industrial application.<sup>42</sup>

### TG analysis

The high thermal stability of ACF samples is one of the most important characteristics for their practical applications. Fig. 6 shows the thermal decomposition of pristine ACFs, DA-ACFs, L-

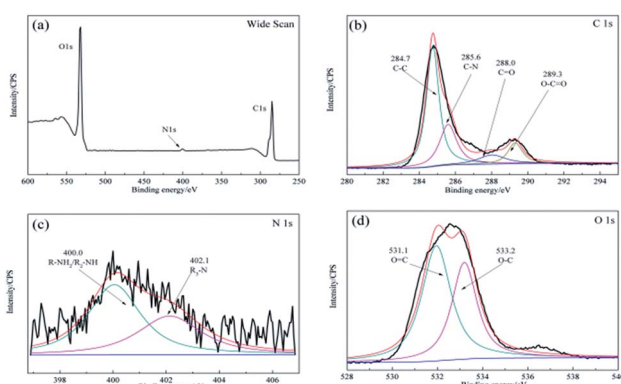


Fig. 3 XPS spectra of the microspheres for LDA-ACFs: (a) wide scan, (b) C 1s, (c) N 1s and (d) O 1s.



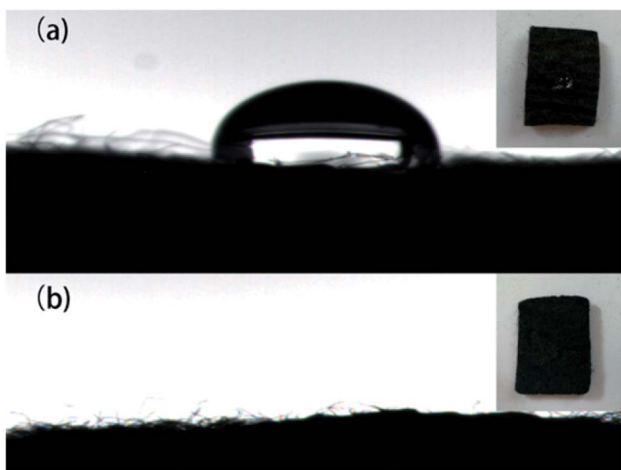


Fig. 5 Photographs of water on (a) ACFs and (b) DA-ACFs.

ACFs, and LDA-ACFs in a nitrogen atmosphere. The weight loss region of the samples below 105 °C was approximately 1%, which demonstrated minimal absorption of physical water to the fibers. Therefore, the large peaks detected between 3500 cm<sup>-1</sup> and 3000 cm<sup>-1</sup> were ascribed to the N–H stretching bands (Fig. 4b and c).

It is well known that pristine ACFs possess good thermal stability.<sup>43</sup> In this study, the ACFs exhibited weight loss of approximately 7% when the temperature reached 800 °C, indicating excellent thermal stability. However, the TG curve of the DA-ACFs showed that a weight loss of approximately 5% occurred from 100 °C to 180 °C, which was caused by vaporization of the water bound to the fibers. DA is thermally stable up to 250 °C, and the mass loss of 11% occurring from 200 °C to 450 °C corresponded to breakdown of the cross-linked surface framework created by grafting of the poly-dopamine coating.<sup>44</sup> Below 200 °C, the weight loss traces of the L-ACFs and LDA-ACFs showed similar thermal behavior to that of the DA-ACFs. In the TG curves of L-ACFs and LDA-ACFs, the weight loss of 15.6% occurring from 200 °C to 300 °C was attributed to decomposition of the protein backbone of immobilized laccase.<sup>45</sup> In

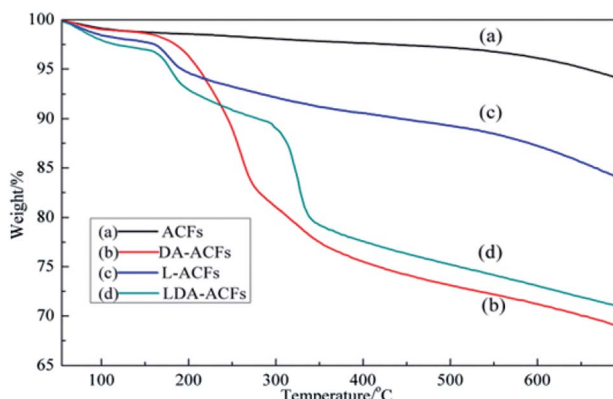


Fig. 6 Thermo-gravimetric curves of (a) ACFs, (b) DA-ACFs, (c) L-ACFs, and (d) LDA-ACFs.

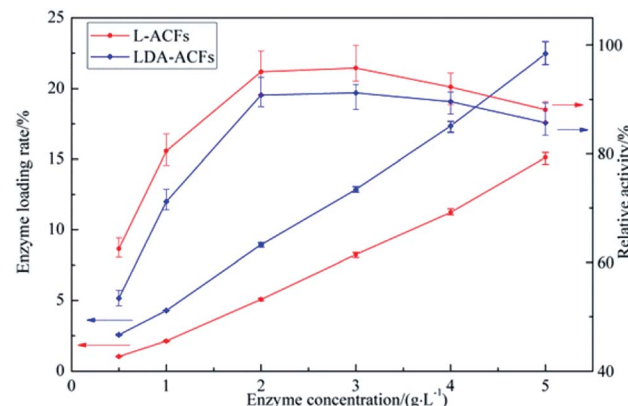


Fig. 7 Enzyme loading rate and relative activity of immobilized laccase with different laccase concentration.

contrast to L-ACFs, the weight loss occurring between 300 and 500 °C in LDA-ACFs was likely attributed to the effect of poly-dopamine.

### Optimization of the immobilization laccase concentration

The protein content loaded on the samples and the relative activity of the immobilized laccase are shown in Fig. 7. The maximal activity of L-ACFs was  $97.1 \pm 2.5 \text{ U g}^{-1}$  (12.86 wt%) when the laccase concentration reached 3 g L<sup>-1</sup> and then declined to levels comparable to that of LDA-ACFs as the laccase concentration continued increasing. This result could be explained by the previous observation that, a high free laccase concentration can enhance the intermolecular steric hindrance, which restrains the diffusion of substrates and products.<sup>46</sup> Therefore, the optimized concentration of laccase used for preparing samples was 2.0 g L<sup>-1</sup> was affected by technical and economic factors, and was used in all other experiments.

### Effect of pH and temperature on enzymatic activity

The optimal pH range for laccase activity is a signature property characteristic of free and immobilized laccase.<sup>3</sup> The optimal pH level of laccase was reported to be approximately 4.0.<sup>47</sup> The different effects of pH on free and immobilized laccases were compared over the pH range of 2.0–8.0. The reactions were monitored at 30 °C for 60 min, and the maximum relative enzymatic activity was defined as 100%. As shown in Fig. 8a, the optimum pH value for free laccase was found to be 4.0, whereas L-ACFs and LDA-ACFs exhibited maximal relative activities at pH 4.5. As the pH increased above 4.0, the relative activity of free laccase decreased sharply, which could be attributed to the change in the redox-potential of the enzymatic reaction and the binding of OH<sup>-</sup> which can block the internal electron transfer in the enzyme.<sup>48</sup> However, the L-ACFs and LDA-ACFs retained relatively higher enzymatic activity over a broad pH ranging from 3.5 to 6.5. This effect might be attributed to the ability of the surface of the carrier to provide a more favorable micro-environment as well as a buffer for the enzyme to undergo H<sup>+</sup> dissociation, which can in turn help alleviate changes in the enzyme conformation that occur during pH changes.<sup>49</sup> In



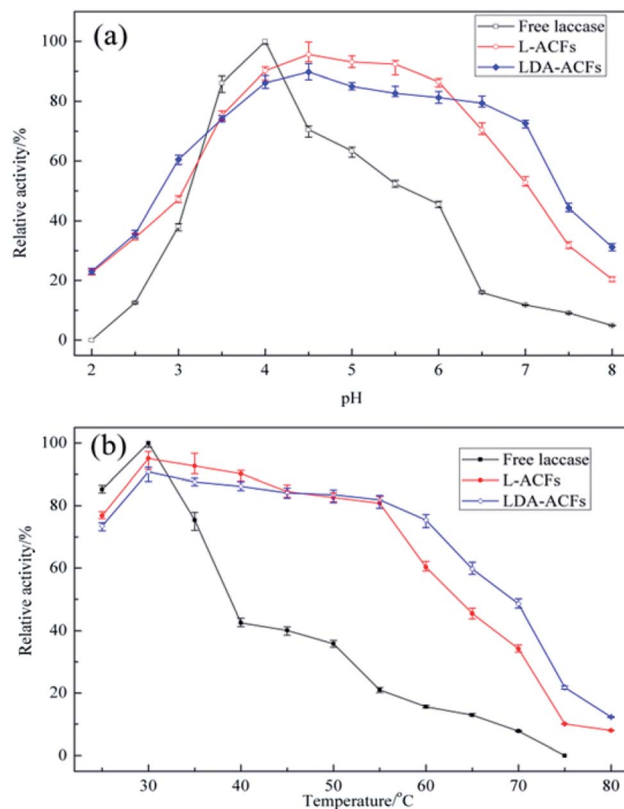


Fig. 8 Effect of pH (a) and temperature (b) on the laccase activities in free and immobilized preparations.

contrast to free laccase, the LDA-ACFs were much more stable over a wide optimum pH range, which could improve its versatility for various applications.

The effect of temperature on the relative activities of laccase is also a vital for bioprocesses, which greatly affects the enzymatic activity and membrane turgidity of cells and yeasts. The effect of temperature on the reactions was monitored between 25 °C and 80 °C. At temperatures above 35 °C, a sharp decline in the relative activity of free laccase was observed, while the immobilized laccase on the ACFs and DA-ACFs exhibited a broader temperature for optimum activity ranging from 30–55 °C, with only 20% loss (Fig. 8b). Remarkably, at 75 °C, the DA-

ACFs still retained more than 20% activity. The immobilized laccase was more stable than that of the free enzyme in the range of 30–55 °C, suggesting that enzyme immobilization effectively stabilized laccase. This finding might be ascribed to the carrier, which can enhance the rigidity of the molecular structure of the laccase and reduce its temperature sensitivity.<sup>46</sup> Indeed, a clear relationship exists between a carrier and an enzyme, and high retention of enzymatic activity is generally obtained with more hydrophilic materials.<sup>50</sup> However, interaction between the carrier and laccase does not allow the enzyme molecules more freely, which results in decreased enzymatic activity.<sup>51</sup>

### Stability of free and immobilized laccase

Several factors contribute to the overall stability of an enzyme, including the thermo-stability, reusability, and storage stability under extreme conditions. The stability of biocatalysts is one of the most important parameters for industrial applications of enzyme, since the technological potential of an enzyme depends on its operational stability, which impacts the overall costs of enzymatic applications.<sup>52</sup>

Thermal stability assays were performed with free and immobilized laccase at 55 °C for 6 h. The thermal stability of free laccase was poor, and the enzymatic activity decreased sharply after incubation at 55 °C for 30 min and lost approximately 90% of its activity after 2 h (Fig. 9a). In contrast, laccase immobilized with the ACFs and DA-ACFs showed high thermal stability, and more than 50% of the enzymatic activity of DA-ACFs remained after 5 h. The main factor responsible for this improvement in thermo-stability might be the interactions between the carrier and laccase, such as hydrogen bonds, hydrophobic interactions, and electrostatic interactions, which can promote further rigidity of the enzyme structure and greater resistance against thermal denaturation.<sup>3</sup>

The operational stability of the immobilized laccase was determined (pH 5.0, 30 °C, 30 min), and the L-ACFs and LDA-ACFs were washed with buffer after each experiment. As shown in Fig. 9b, the relative activity of immobilized laccase decreased with increased use, and 60% and 40% of the original activity of the LDA-ACFs and L-ACFs was retained after 6 cycles, respectively. This observation could be explained by the denaturation of enzyme on the surfaces of carriers, as well as enzyme

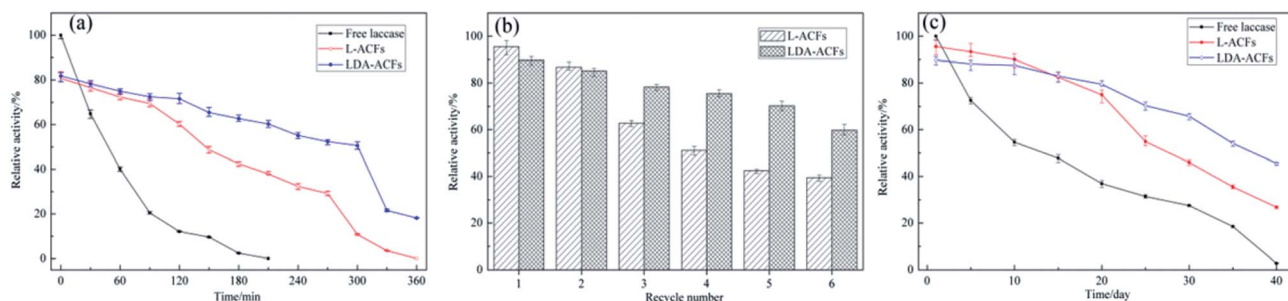


Fig. 9 Stabilities of free and immobilized preparations: (a) thermal stability of free and immobilized laccase incubated for 6 h, (b) operational stability of immobilized laccase (pH 5.0, 30 °C) incubated for 0.5 h, (c) storage stability of free and immobilized laccase (pH 5.0, 4 °C) incubated for 40 days.

Table 2 Kinetic parameters of free and immobilized laccase

Enzyme	$V_{\max}$ (mg (mL min) $^{-1}$ )	$K_m$ (mg mL $^{-1}$ )
Free laccase	16.47 $\pm$ 0.74	0.59 $\pm$ 0.02
L-ACFs	9.10 $\pm$ 0.44	0.70 $\pm$ 0.03
LDA-ACFs	6.37 $\pm$ 0.26	0.65 $\pm$ 0.03

leakage from carriers during the reactions.<sup>45</sup> It has also been suggested that subsequent immobilization of these aggregates would render them permanently insoluble while maintaining their catalytic activity.<sup>17</sup>

The stabilities of the free and immobilized laccase were tested during storage in an aqueous solution (0.5 mM buffer) at 4 °C in the pH of 5.0. As shown in Fig. 9c, the relative activity of free laccase decreased significantly after a 10 day incubation, and lost virtually all activity after 40 days. However, the stability of the immobilized laccase was much higher compared to that of the free laccase, indicating that the LDA-ACFs might remain active over several months. This result can be attributed to the higher concentration of binding sites on the carrier, which would increase the binding density to in turn reduce the enzyme mobility, thereby increasing the enzyme stability with the multivalent interactions.<sup>53</sup>

### Kinetic analysis of free and immobilized laccase

The Michaelis constant ( $K_m$ ) is an important parameter for measuring the affinity of an enzyme with its substrate, and the  $V_{\max}$  value defines the maximum reaction velocity. A lower  $K_m$  value indicates a higher binding ability for the substrate. As shown in Table 2 and Fig. 10, the  $K_m$  values of the immobilized laccase samples were slightly higher than those of free laccase, which indicates that the enzymatic affinity for ABTS was less impacted by the immobilization procedure due to the small diameter of the carriers.<sup>54</sup> However, the  $V_{\max}$  values of the L-ACFs and LDA-ACFs were determined to be 9.10 mg (mL min) $^{-1}$  and 6.37 mg (mL min) $^{-1}$ , respectively, which were markedly lower than that of free laccase at 16.47 mg (mL min) $^{-1}$ . This change

may be ascribed to an increasing diffusion limit of substrates and laccase caused by the carriers.<sup>55</sup>

## Conclusion

The ultimate goal of this work was to achieve laccase immobilization on the surface of ACFs, which was accomplished *via* modification using oxidative self-polymerization. Compared with the traditionally synthesized carrier materials, the DA-ACFs exhibited superior performance on account of their large surface area, and high biocompatibility and hydrophilicity as determined through SEM, XPS, ATR-FTIR, and TG measurements. The properties of immobilized laccase with DA-ACFs were enhanced compared to those of free laccase and L-ACFs, particularly with respect to high enzyme loading and stability.

In summary, poly-dopamine based ACFs have gained increasing attentions as novel enzyme supports due to their good biocompatibility and simple process used for immobilization. Furthermore, ABTS was used as a model substrate for immobilization in this study, and a catalytic mechanism is proposed. We therefore expect that L-ACFs and LDA-ACFs are promising research tools that can replace traditional chemical-conversion methods used in academic and industrial laboratories because of their high efficiency, economic considerations, and sustainability.

## Conflicts of interest

There are no conflicts to declare.

## Acknowledgements

This work was financially supported by the Young People Fund of Nantong Science (No. WQ2016001). The authors are also thankful for the support of the Fundamental Research Funds for the Nantong Universities (No. 17ZH158). It is also funded by Nantong Applied Research Program (No. GY12016031).

## Notes and references

- 1 A. I. Yaropolov, O. V. Skorobogat'ko, S. S. Vartanov and S. D. Varfolomeyev, *Appl. Biochem. Biotechnol.*, 1994, **49**, 257–280.
- 2 M. Asgher, A. Ijaz and M. Bilal, *Turk. J. Biochem.*, 2016, **41**, 26–36.
- 3 R. P. Georgiou, E. P. Tsiakiri, N. K. Lazaridis and A. A. Pantazaki, *J. Environ. Chem. Eng.*, 2016, **4**, 1322–1331.
- 4 H. F. Sun, H. Yang, W. W. Huang and S. J. Zhang, *J. Colloid Interface Sci.*, 2015, **450**, 353–360.
- 5 C. A. Gasser, E. M. Ammann, P. Shahgaldian and P. F. Corvini, *Appl. Microbiol. Biotechnol.*, 2014, **98**, 9931–9952.
- 6 M. D. Stanescu, M. Fogorasi, B. L. Shaskolskiv, S. Gavrilas and V. I. Lozinsky, *Appl. Biochem. Biotechnol.*, 2010, **160**, 1947–1954.
- 7 O. Saoudi, N. Ghaouar, S. Bensalah and T. Othman, *Biochem. Biophys. Rep.*, 2017, **11**, 19–26.

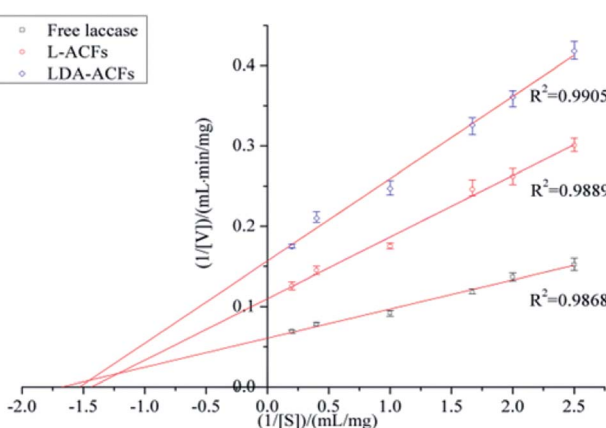


Fig. 10 Lineweaver–Burk plots for free and immobilized laccase.



8 J. Kulys, R. Vidziunaite and P. Schneider, *Enzyme Microb. Technol.*, 2003, **32**, 455–463.

9 N. Nasoohi, K. Khajeh, M. Mohammadian and B. Ranjbar, *Int. J. Biol. Macromol.*, 2013, **60**, 56–61.

10 R. Abejon, M. P. Belleville and J. S. Marcano, *Sep. Purif. Technol.*, 2015, **156**, 183–199.

11 A. O. Shalash, A. M. Molokhia and M. A. Elsayed, *Eur. J. Pharm. Biopharm.*, 2015, **96**, 291–303.

12 J. Zdarta, A. S. Meyer, T. Jesionowski and M. Pinelo, *Catalysts*, 2018, **8**, 92.

13 A. Rekuc, P. Kruczkiewicz, B. Jastrzembska, J. Liesiene, W. P. Czoch and J. Bryjak, *Int. J. Biol. Macromol.*, 2008, **42**, 208–215.

14 J. Bryjak, P. Kruczkiewicz, A. Rekuc and W. P. Czoch, *Biochem. Eng. J.*, 2007, **35**, 325–332.

15 U. Guzik, K. H. Kocurek and D. Wojcieszynska, *Molecules*, 2014, **19**, 8995–9018.

16 T. Jesionowski, J. Zdarta and B. Krajewska, *Adsorption*, 2014, **20**, 801–821.

17 R. A. Sheldon, *Adv. Synth. Catal.*, 2007, **349**, 1289–1307.

18 A. S. Bommarius and M. F. Paye, *Chem. Soc. Rev.*, 2013, **42**, 6534–6565.

19 C. L. Mangun, K. R. Benak, J. Economy and K. L. Foster, *Carbon*, 2001, **39**, 1809–1820.

20 X. P. Zhang, X. Zhao, J. Q. Hu, C. H. Wei and H. T. Bi, *J. Hazard. Mater.*, 2011, **186**, 1816–1822.

21 H. M. Zuo, H. Zhang, X. X. Zhang and N. Han, *J. Appl. Polym. Sci.*, 2013, **130**, 2619–2623.

22 C. L. Mangun, J. A. DeBar and J. Economy, *Carbon*, 2001, **39**, 1689–1696.

23 H. Q. Rong, Z. Y. Ryu, J. T. Zheng and Y. L. Zhang, *Carbon*, 2002, **40**, 2291–2300.

24 D. Q. Mo and D. Q. Ye, *Surf. Coat. Technol.*, 2009, **203**, 1154–1160.

25 J. S. Moon, K. K. Park, J. H. Kim and G. Seo, *Appl. Catal. A*, 2000, **201**, 81–89.

26 D. P. Dowling, I. S. Miller, M. Ardhaoui and W. M. Gallagher, *J. Biomater. Appl.*, 2011, **26**, 327–347.

27 L. Wang, N. Liu, Z. Guo, D. P. Wu, W. W. Chen, Z. Chang, Q. P. Yuan, M. Hui and J. S. Wang, *Materials*, 2016, **9**, 206.

28 X. Yanga, L. Hua, H. Gong and S. N. Tan, *Anal. Chim. Acta*, 2003, **478**, 67–75.

29 H. Lee, S. M. Dellatore, W. M. Miller and P. B. Messersmith, *Science*, 2007, **318**, 426–430.

30 J. F. Shi, C. Yang, S. H. Zhang, X. L. Wang, Z. Y. Jiang, W. Y. Zhang, X. K. Song, Q. H. Ai and C. Y. Tian, *ACS Appl. Mater. Interfaces*, 2013, **5**, 9991–9997.

31 C. Yang, H. Wu, J. F. Shi, X. L. Wang, J. J. Xie and Z. Y. Jiang, *Ind. Eng. Chem. Res.*, 2014, **53**, 12665–12672.

32 C. C. Zhang and P. F. Han, *Text. Aux.*, 2017, **34**, 21–23.

33 R. Pang, M. Z. Liu and C. D. Zhang, *Talanta*, 2015, **131**, 38–45.

34 R. Xu, J. Y. Cui, R. Z. Tang, F. T. Li and B. R. Zhang, *Chem. Eng. J.*, 2017, **326**, 647–655.

35 J. H. Lin, Q. J. Lai, Y. J. Liu, S. Chen, X. Y. Le and X. H. Zhou, *Int. J. Biol. Macromol.*, 2017, **102**, 144–152.

36 D. Zhang, M. F. Deng, H. B. Cao, S. P. Zhang and H. Zhao, *Green Energy & Environment*, 2017, **2**, 393–400.

37 R. Sa, Y. Yan, Z. H. Wei, L. Q. Zhang, W. C. Wang and M. Tian, *ACS Appl. Mater. Interfaces*, 2014, **6**, 21730–21738.

38 H. Lee, N. F. Scherer and P. B. Messersmith, *Proc. Natl. Acad. Sci.*, 2006, **103**, 12999–13003.

39 J. K. Gao, Y. J. Jiang, J. S. Lu, Z. Hai, J. J. Deng and Y. Chen, *Sci. Rep.*, 2017, **1**, 1–9.

40 Q. Zhou, Q. Zhang, P. Wang, C. Deng, Q. Wang and X. R. Fan, *Fibers Polym.*, 2017, **18**, 1478–1485.

41 L. J. Zhu, Y. L. Lu, Y. Q. Wang, L. Q. Zhang and W. C. Wang, *Appl. Surf. Sci.*, 2015, **258**, 5387–5393.

42 L. A. Belyaeva, P. M. G. V. Deursen, K. I. Barbetsea and G. F. Schneider, *Adv. Mater.*, 2018, **30**, 1703274.

43 X. F. Yan, S. J. Xu, Q. Wang and X. R. Fan, *Nanoscale Res. Lett.*, 2017, **12**, 590.

44 H. J. Kang, X. R. Liu, S. F. Zhang and J. Z. Li, *RSC Adv.*, 2017, **7**, 24140–24148.

45 S. L. Pang, Y. W. Wu, X. Q. Zhang, B. N. Li, J. O. Yang and M. Y. Ding, *Process Biochem.*, 2016, **51**, 229–239.

46 F. Wang, C. Guo, H. Z. Liu and C. Z. Liu, *J. Chem. Technol. Biotechnol.*, 2008, **83**, 97–104.

47 A. P. M. Tavares, C. G. Silva, G. Drazic, A. M. T. Silva, J. M. Loureiro and J. L. Faria, *J. Colloid Interface Sci.*, 2015, **454**, 52–60.

48 M. B. Asif, F. I. Hai, J. W. Hou, W. E. Price and L. D. Nghiem, *J. Environ. Manage.*, 2017, **201**, 89–109.

49 G. H. Li, A. G. Nandgaonka, K. Y. Lu, W. E. Krause, L. A. Lucia and Q. F. Wei, *RSC Adv.*, 2016, **6**, 41420–41427.

50 D. Kraemer, H. Plainer, B. Sproessier, H. Uhlig and R. Schnee, *US Pat.* 4839419, 1989.ss.

51 S. Sasmaz, S. Gedikli, P. Aytar, G. Gungormedi, A. Gabuk, E. Hur, A. Unal and N. Kolankaya, *Appl. Biochem. Biotechnol.*, 2011, **163**, 346–361.

52 M. Tahern, M. Naghdi, S. K. Brar, E. J. Knystautas, M. Verma and R. Y. Surampalli, *Sci. Total Environ.*, 2017, **605–606**, 315–321.

53 J. P. Hu, B. N. Yuan, Y. M. Zhang and M. H. Guo, *RSC Adv.*, 2015, **5**, 99439–99447.

54 M. Mohammadi, M. A. As'habi, P. Salehi, M. Yousefi, M. Nazari and J. Brask, *Int. J. Biol. Macromol.*, 2018, **109**, 443–447.

55 S. Rouhani, A. Rostami and A. Salimi, *RSC Adv.*, 2016, **6**, 26709–26718.

